

N 9 2 - 1 0 9 3 3

Impact Cratering Calculations.

Thomas J. Ahrens, J.D. O'Keefe, C. Smither and T. Takata, Seismological Laboratory, California Institute of Technology, Pasadena, CA.

In the course of carrying out finite difference calculations¹, we discovered that for large craters, a previously unrecognized type of crater (diameter) growth occurred which we have called "lip wave propagation." This type of growth is illustrated in Figure 1 for an impact of a 1000 km (2a) silicate bolide at 12 km/sec (U) onto a silicate half-space at earth gravity (1 g). The von Misses crustal strength is 2.4 kbar. The motion at the crater lip associated with this wave type phenomenon is up, outward, and then down, similar to the particle motion of a surface wave. In Fig. 1, we see that the crater diameter has grown from $d/a \sim 25$ to $d/a \sim 4$ via lip propagation from $Ut/a=5.56$ to 17.0 during the time when rebound occurs.

We are starting to use a new code completely written at Caltech under this program to study partitioning of energy and momentum and cratering efficiency with self gravity for finite-sized objects rather than the planetary half-space problems discussed above. These are important and fundamental subjects which can be addressed with SPH codes. The Smoothed Particle Hydrodynamics (SPH) method of Gingold and Monaghan² has been used to model various problems in astrophysics and planetary physics.

Our initial work demonstrates that the energy budget for normal and oblique impacts are distinctly different than earlier calculations for silicate projectile impact on a silicate half space³. As illustrated in Fig. 2, energy budgets depend on impact geometry. We have not yet varied relative projectile size. For Fig. 2, the target radius was set at 1700 km; the impactor radius was 40% of the target radius. Both normal and oblique impacts were modeled for impact velocities of 10 and 20 km/sec. The fraction of the total energy in the kinetic energy of the impactor and target and the internal energy of the two bodies are plotted with respect to normalized time $\tau=Ut/a$, where U is the impact velocity, a is the impactor radius, and τ is the elapsed time after impact. Note that the amount of the total energy remaining in the kinetic energy of the impactor is much greater for the oblique case than in the normal impact case.

Motivated by the first striking radar images of Venus obtained by Magellan, we have been studying the effect of the atmosphere on impact cratering. In order to further quantify the processes of meteor break-up and trajectory scattering upon break-up, we have examined the reentry physics of meteors striking Venus' atmosphere versus that of the Earth. Because of the usual density gradient of an assumed adiabatic atmosphere, there is a strong tendency for the atmospheres, especially Venus, to "refract" incoming, obliquely incident projectiles toward a trajectory nearly normal to the planet. This "refraction" effect is a strong function of initial impact angle, the atmosphere scale height, as well as mass and velocity (Fig. 3). Because of the marked asymmetry of ejecta patterns on Venus, which are presumed to have been generated by atmospheric effects, the angular distribution of incoming projectiles needs to be understood. We are presently studying this effect.

REFERENCES: ¹O'Keefe and Ahrens (1977). *Proc. 8th Lunar Sci. Conf.*, 3357-3375.
²Gingold, R.A. and Monaghan, J.J. (1982). *J. Computational Physics* **46**, 429-453.
³Ahrens *et al.* (1989). *Origin and Evolution of Planetary and Satellite Atmospheres*, 328-385.

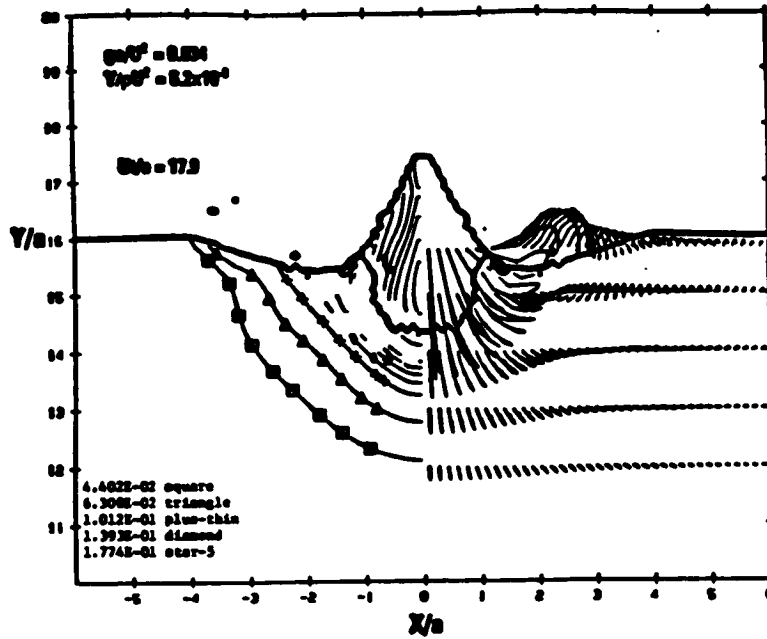


Fig. 1: Displacement history and internal energy induced by 1000 km, diameter, 12 km/sec 2.7 g/cm^3 silicate impact striking silicate planet with 2.4 kbar von Mises yield strength. Depth, D , and radius, d , are normalized by projectile radius, a . Nearly complete rebound has occurred at $Ut/a=17.9$ and shallow crater is still increasing its outer radius from its initial transient radius of $\sim 2.5 a$ to $\sim 4 a$. On left are contours of internal energy in ev/g , whereas on the right we show total displacement history for a series of markers in the initial spherical projectile and target.

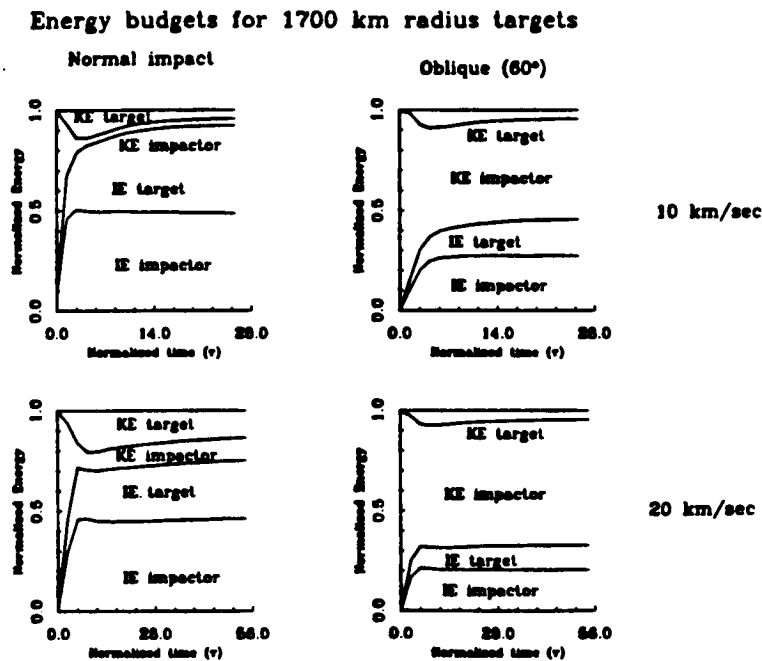


Fig.2: Partitioning between kinetic energy (KE) and internal energy (IE) budgets versus normal (left) and obliquely (right) at 10 (upper) and 20 (lower) km/sec by 680 km radius impactor.

Atmospheric Effect on the Trajectory of Meteor

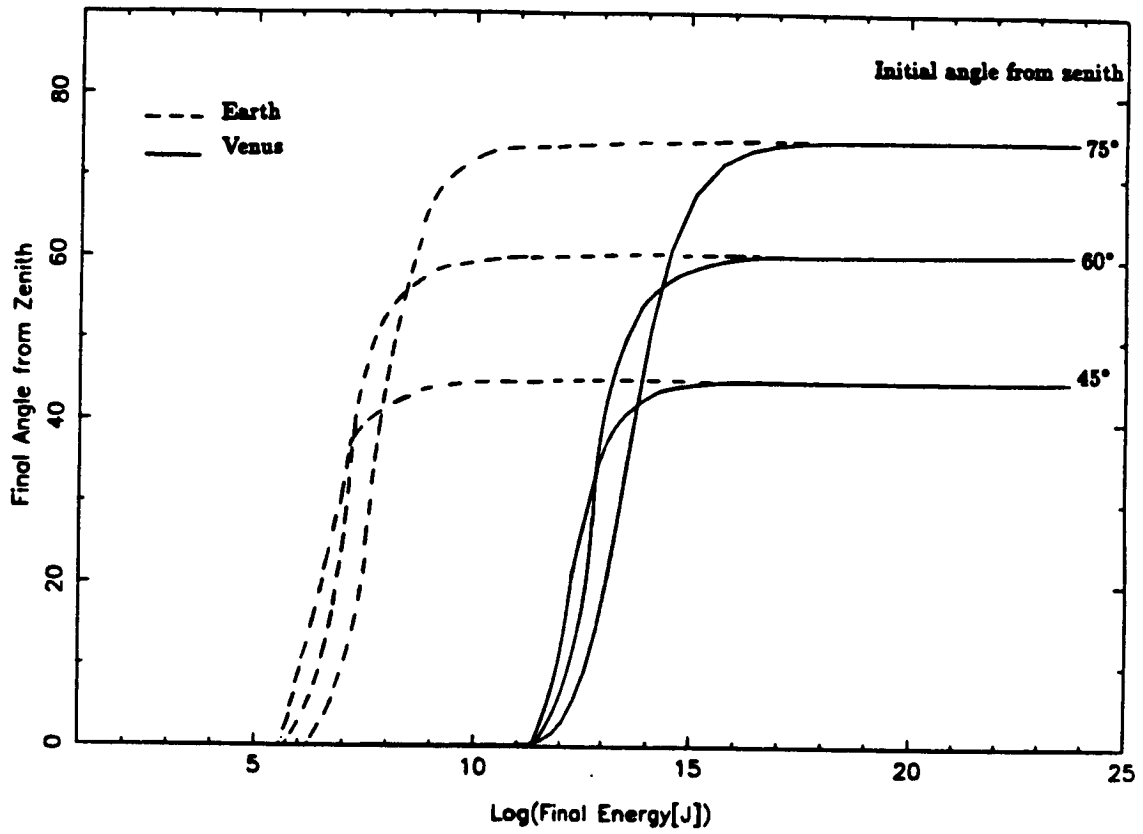


Fig. 3: Bolide-impact angle versus bolide energy for different orientations from the zenith for Earth and Venus atmospheres. Drag coefficient of 1.2, heat of vaporization and ionization of 30 MJ/kg and heat transfer coefficient 0.5 are assumed (Takata and Ahrens, unpublished).